New Journal of Physics
The open access journal for physics

Impact of extended preplasma on energy coupling in kilojoule energy relativistic laser interaction with cone wire targets relevant to fast ignition

T Yabuuchi[1,9], R Mishra[1], C McGuffey[1], B Qiao[1], M S Wei[2], H Sawada[1,3], Y Sentoku[3], T Ma[1,4], D P Higginson[1,4], K U Akli[2], D Batani[5], H Chen[4], L A Gizzi[6], M H Key[4], A J Mackinnon[4], H S McLean[4], P A Norreys[7], P K Patel[4], R B Stephens[2], Y Ping[4], W Theobald[8], C Stoeckl[8] and F N Beg[1,10]

[1] Center for Energy Research, University of California, San Diego, La Jolla, CA 92093, USA
[2] General Atomics, San Diego, CA 92121, USA
[3] Department of Physics, University of Nevada, Reno, NV 89557-0220, USA
[4] Lawrence Livermore National Laboratory, Livermore, CA 94551, USA
[5] Centre Lasers Intenses et Applications, Université Bordeaux 1, 351, Talence Cedex, France
[6] Intense Laser Irradiation Laboratory, INO-CNR, Pisa, Italy
[7] STFC Rutherford Appleton Laboratory, Didcot, UK
[8] Laboratory for Laser Energetics, University of Rochester, Rochester, NY 14623, USA
E-mail: fbeg@ucsd.edu

New Journal of Physics **15** (2013) 015020 (14pp)
Received 17 September 2012
Published 25 January 2013
Online at http://www.njp.org/
doi:10.1088/1367-2630/15/1/015020

Abstract. Cone-guided fast ignition laser fusion depends critically on details of the interaction of an intense laser pulse with the inside tip of a cone. Generation of relativistic electrons in the laser plasma interaction (LPI) with a gold cone and their subsequent transport into a copper wire have been studied using a kJ-class

[9] Current address: Osaka University, Osaka 565-0871, Japan.
[10] Author to whom any correspondence should be addressed.

intense laser pulse, OMEGA EP (850 J, 10 ps). We observed that the laser-pulse-energy-normalized copper Kα signal from the Cu wire attached to the Au cone is significantly reduced (by a factor of 5) as compared to that from identical targets using the Titan laser (150 J, 0.7 ps) with 60$\times$ less energy in the prepulse. We conclude that the decreased coupling is due to increased prepulse energy rather than 10 ps pulse duration, for which this effect has not been previously explored. The collisional particle-in-cell code PICLS demonstrates that the preformed plasma has a significant impact on generation of electrons and their transport. In particular, a longer scale length preplasma significantly reduces the energy coupling from the intense laser to the wire due to the larger offset distance between the relativistic critical density surface and the cone tip as well as a wider divergence of source electrons. We also observed that laser-driven plasma ionization increase in the LPI region can potentially alter the electron density profile during the laser interaction, forcing the electron source to be moved farther away from the cone tip which contributes to the reduction of energy coupling.

Contents

1. Introduction

Conventional laser driven inertial confinement fusion requires stringent laser or x-ray irradiation uniformity and fuel shell smoothness to create a central hot spot in spite of hydrodynamics instabilities during compression. These requirements are relaxed in the fast ignition (FI) approach due to its separation of compression and heating phases [1]. The required fast heating of the compressed fuel can be achieved with high energy particles, electrons or ions, which could be created by a high energy, intense laser pulse ($\sim 10^{20}$ W cm^{-2}) [2], and which deposit their energy in the pre-compressed fuel. Several approaches have been proposed to achieve efficient heating of the compressed plasma with fast electrons: laser hole-boring [3], super-penetration [4] and guiding by a re-entrant cone [5]. Cone-guided FI has attracted much attention due to its successful demonstration of a 10^3 times increase in neutron yield from the deuterium–deuterium fusion reaction using a sub-picosecond heating pulse with 500 J energy into a reentrant gold cone on a CD shell, with $\sim$20% coupling efficiency to the imploded

core [6]. More recent work at the OMEGA EP (extended performance) laser has however shown much lower coupling efficiency (3.5%) [7] with a higher energy laser pulse. The reduction was attributed to the presence of preplasma which has been investigated using the Titan laser [8] as well as the LULI laser [9]. The present work explores possible causes using the same laser as in [7] yet with higher prepulse.

The detailed underlying physics of the fast electron heating process in cone-guided FI requires a systematic investigation including (i) interactions of the laser pulse with the cone, (ii) fast electron transport inside the cone tip, (iii) transport into the coronal plasma and high density core behind the cone tip, and (iv) core plasma heating by the fast electrons. Several experiments have been carried out using sub-picosecond laser pulses with energies up to ∼500 J to address the first two issues [8–13]. However, data with higher energies and ∼10 ps laser pulses did not exist until the completion of OMEGA EP, a kilo-joule class short pulse laser facility[14], which has enabled us to extend the experimental study from sub-picosecond pulse to FI-relevant laser pulse durations (i.e. ∼10 ps) while maintaining high enough laser intensities ($I \geqslant 10^{19}$ W cm^{-2}). In a recent computational study [15], plasma profiles and hot electron generation were found to evolve significantly over several picoseconds. Furthermore, in a gold plasma such as the one in this paper, dynamic ionization will play an important role for longer pulses which will also significantly modify the density profile during the laser plasma interaction (LPI) with 10 ps pulses compared to 1 ps. Published experimental data concerning electron generation and/or energy coupling from laser solid interactions with 10 ps pulses to date have been limited to a planar geometry study [16], a study in conical geometry with low energy (70 J) [17], and another at high energy which did not address the electron behavior [7]. Kilojoule high intensity pulses generated by existing laser technologies have considerable energy in a prepulse or plateau lasting a few ns before the main pulse. The plasma created by this early energy (typically 10s to 100s of mJ from a 1 kJ pulse) can substantially affect the laser energy absorption, electron generation and transport as seen in recent sub-scale FI experiments [7, 18]. In addition, the 10 ps pulse duration is sufficiently long as to allow density profile steepening or plasma expansion during the high intensity LPIs [19, 20]. It is extremely challenging to model the LPI over such long pulse duration and plasma scale length as it warrants significant computational resources. Therefore, it is essential to conduct an experimental study that isolates the fast electron generation and transport physics without the complexity of the density and temperature variation in the compressed core.

In this article, we report the experimental study of fast electron generation in a gold cone and energy coupling into the attached wire target using a 10 ps laser pulse with energies up to 810 J and also the computational study of LPI and fast electron generation and transport in such targets including dynamic ionization processes in the cone-wire target. This work focuses on implications for FI, but the cone-wire configuration and findings here may be of interest to other applications that depend on the spatial, angular and energy distribution of fast electrons, such as sheath acceleration of ions [21], and has implications for applications employing a conical target such as laser intensity enhancement [22, 23], neutron generation [24] and electron guiding [25]. The experiment uses the same methodology as recently reported work with the 150 J Titan laser facility [8], but extends the study to a new regime of longer pulse duration and high energy. Additionally, particle-in-cell (PIC) modeling is presented, which quantifies the loss mechanisms of hot electrons due to large beam divergence and geometric considerations and also demonstrates the importance of ionization in the LPI region, which can significantly alter the density profile, particularly in gold.

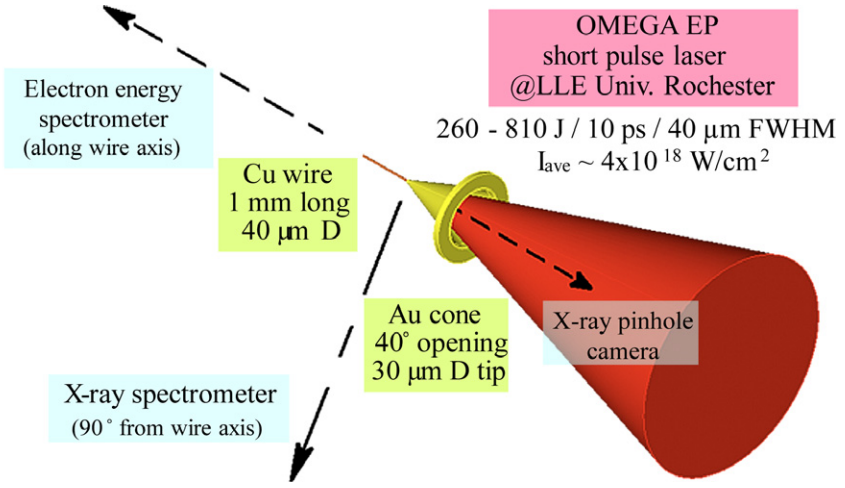

Figure 1. Schematic overview of experimental setup in the OMEGA EP target chamber.

2. Experimental details

The experiment was performed using OMEGA EP's kilojoule-class 10 ps laser at the Laboratory for Laser Energetics at the University of Rochester [14]. The EP short pulse beam was focused into the Au cone target with 80% of the beam energy in a ~25 μm radius spot. The energy of the beam was varied from 250 to 810 J with a full width half maximum pulse duration of ~10 ps. The average laser intensity within the spot was 4×10^{18} W cm^{-2}, and the peak intensity was ~10^{19} W cm^{-2} for the 810 J shot, with ~500 mJ in the pedestal (3 ns long). Fast electron generation and the transport through the cone tip were studied using a Cu wire attached to the cone tip. The cone-wire target schematic is shown in figure 1. The target consisted of a 1.0 mm long, 40 μm diameter Cu wire attached to a Au cone with 40° full opening angle, 51 μm tip outer diameter, and 5–10 μm tip thickness. The interaction of the laser and the cone tip produced energetic electrons, of which a fraction transported through the cone tip into the attached wire inducing the 8.0 keV Cu Kα x-rays. The Cu Kα yield was measured with a highly oriented pyrolytic graphite (HOPG) crystal spectrometer [26], which was absolutely calibrated with a single-photon counting camera. The spectrometer was oriented perpendicular to the wire axis. X-ray attenuation in the Cu wire was taken into account in analysis of the data. In addition, thermal plasma emission inside the cone was monitored with a time-integrated x-ray pinhole camera [27], and the spectrum of electrons escaping along the wire axis was measured with an electron spectrometer [28].

The results of the experiment are compared here with similar cone-wire experiments performed on the Titan laser system at the Lawrence Livermore National Laboratory with 150 J pulse energy and 0.7 ps pulse duration in ~7 μm beam spot (see [13] for details of the laser system). The time-integrated pedestal energy prior to the main pulse was ~8 mJ on a typical 150 J shot. The HOPG spectrometer also used at Titan to record Cu Kα emission from the wire had the same design as the one at OMEGA EP so that the data taken at both facilities can be directly compared.

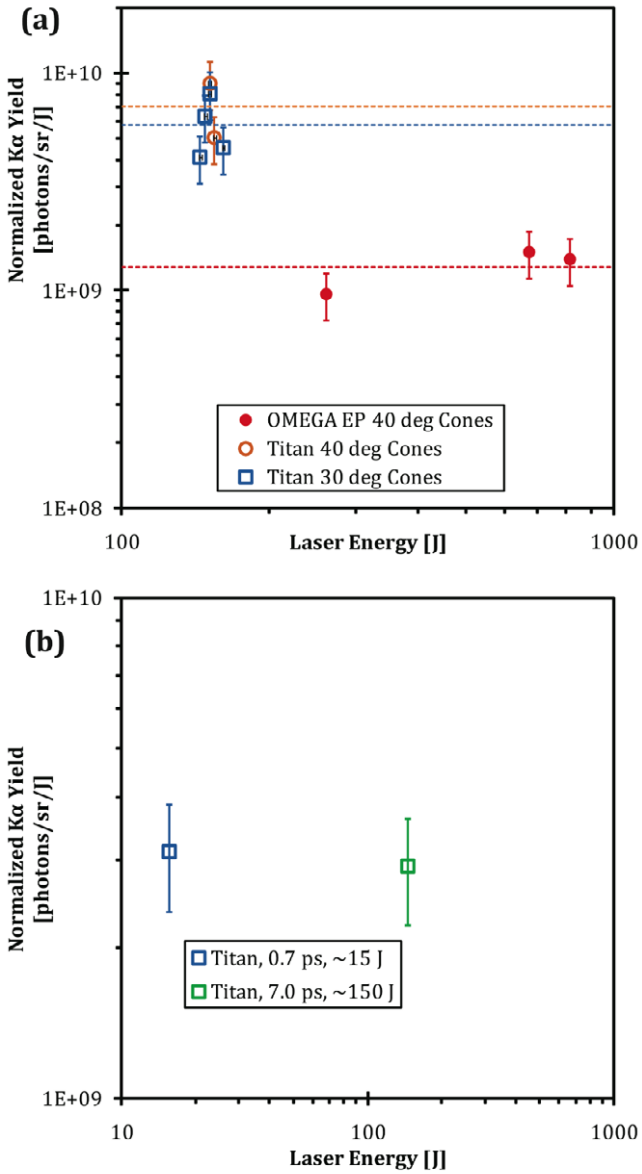

Figure 2. Cu Kα yield from the wire observed with the HOPG spectrometer. (a) Solid circles are taken in OMEGA EP experiments. Open symbols are data from Titan experiments: squares are from similar 30° cone targets and circles are from 40° cone targets identical to those used on OMEGA EP. The average value of each set is shown as a dashed horizontal line. The attenuation of the x-ray signal by the wire is accounted for. (b) The energy-normalized yield versus energy with fixed intensity on Titan including the sub-picosecond case and 7 ps pulse duration.

3. Experimental results

Figure 2(a) shows the measured total Cu Kα yields normalized to laser energy obtained at OMEGA EP (solid red circles) by varying the laser energy (260–810 J) with fixed pulse duration

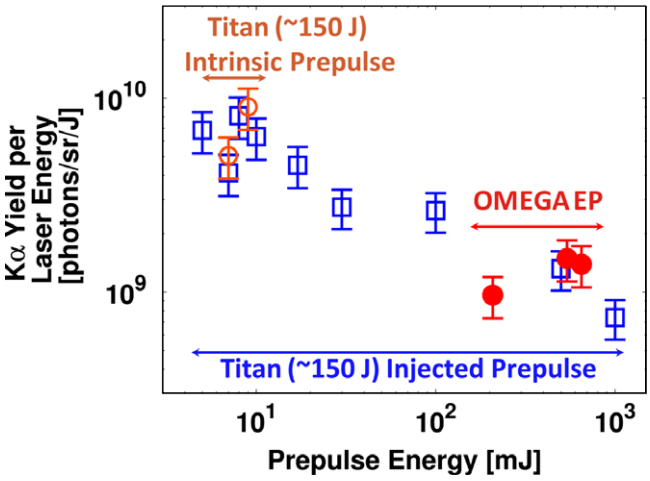

Figure 3. Cu Kα yield normalized to main pulse energy showed a consistent trend as a function of prepulse energy whether the prepulse was Titan's intrinsic prepulse (open circles), an externally injected prepulse on Titan (open squares) or OMEGA EP's intrinsic prepulse (solid circles).

(10 ps) as well as in sub-picosecond scale experiments performed at the Titan laser facility at lower energy (150 J) but similar intensity using the same targets (cone opening angle 40°) shown as open circles. Also shown in this figure is the comparison between two different cone-opening angles (30° and 40°) on the Titan laser. In figure 2(b), the normalized yield from a different set of shots is plotted for two different pulse duration and energy cases with fixed intensity on the Titan laser. These two plots indicate that fast electron produced absolute Kα yield increased almost linearly with the laser energy on OMEGA EP, i.e. the laser-energy-normalized Kα yield was constant, and was insensitive to the change in cone angle of 30° or 40° and to pulse duration over a factor of 10 increase at similar laser intensity ($\sim 1.0 \times 10^{19}$ W cm^{-2}). However, the observed normalized Kα yield at the OMEGA EP experiment was lower than the average value at Titan by a factor of 5.3 ± 1.1.

The lower normalized Kα yield on OMEGA EP, indicative of lower energy coupling efficiency to the Cu wire (and reduced conversion efficiency to the core in FI), can be explained as a direct consequence of preplasma effect. Figure 3 shows the normalized yields from both facilities as a function of prepulse energy. The prepulse energy values for the three OMEGA EP shots plotted in figure 3 are found by multiplying the main pulse energy by a constant coefficient based on reference shots in which the intrinsic prepulse energy was found to be proportional to the main pulse energy. Besides the two cases of the facilities' intrinsic prepulse levels, an external prepulse was injected for a series of shots on the Titan laser with the prepulse energy varied to span the two intrinsic cases (the same experimental campaign as described in [8]). The normalized yield is seen to be clearly dependent upon prepulse energy and consistent between the two facilities when prepulse energy was similar. The intrinsic prepulse pedestal duration is another parameter relevant to preplasma and was similar at the two facilities (~3 ns).

Simulations using the radiation hydrodynamics code HYDRA [29] (in two-dimensional (2D) cylindrical geometry) confirm that the intrinsic 500 mJ prepulse in the 810 J OMEGA EP shot (larger than that of Titan laser by a factor of ~60) creates a large scale preplasma that fills the inside of the gold cone (figure 4(a), top). The preplasma scale length was estimated to be 35 μm near the critical density region, which was about 130 μm from the initial cone tip

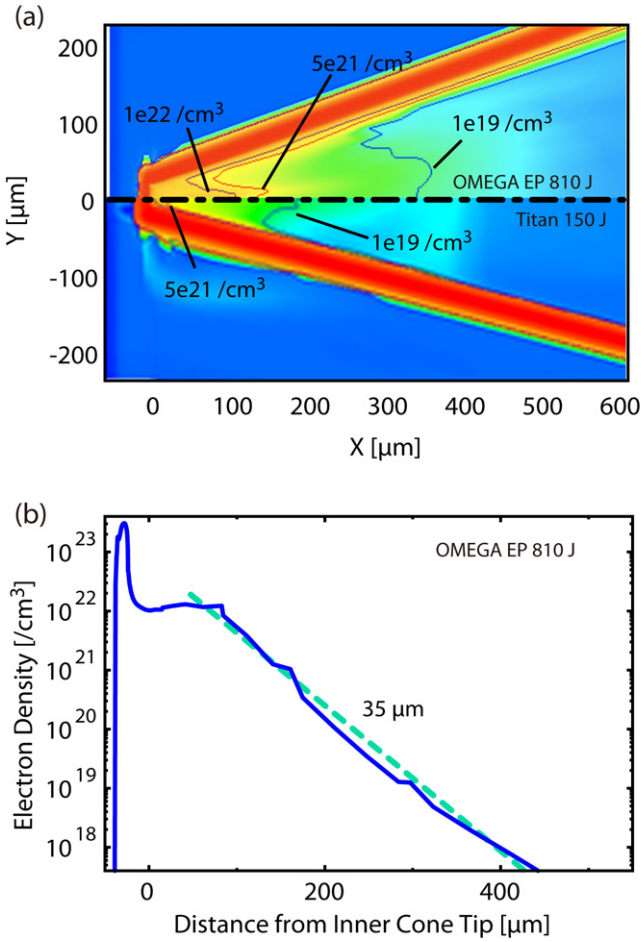

Figure 4. (a) 2D electron density profiles of the preformed plasma inside the cone simulated with a radiation hydrodynamics code HYDRA when the main pulse arrives at the target. The top half (above the dashed line) shows the profile in 40° opening cone under the OMEGA EP condition with 500 mJ class pedestal. The bottom half shows the density profile with 8 mJ prepulse on Titan in the 30° cone. (b) A lineout of the plasma electron density along the cone axis in the case of OMEGA EP. The dashed line (light blue) is the best fit of the profile with an exponential function, which provides the scale length of 35 μm. In both figures, the horizontal axis is given as the distance measured from the inner cone tip.

position. The distance was about four times the offset found in the simulated preplasma density profile with the Titan intrinsic prepulse condition (figure 4(a), bottom). The large extent of the preplasma on OMEGA EP is evident in the x-ray pinhole image shown in figure 5 where the estimated x-ray spot size was about 260 μm. Based on the target geometry, it is concluded that the x-rays were emitted from the preformed plasma up to ~350 μm from the cone tip, where the preplasma density was about 1% of the critical density according to the HYDRA calculation (figure 4(a), top).

The presence of significant pre-formed plasma inside the cone is also consistent with the observed vacuum fast electron spectra, shown in figure 6; they had high spectral-slope-temperatures (1.6 and 3.1 MeV for 260 and 810 J, respectively) compared to the ponderomotive

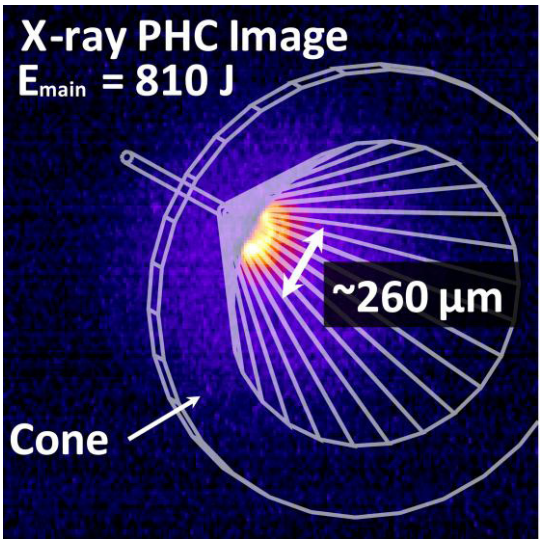

Figure 5. Image of x-ray emission (up to 7 keV) from the interactions between the OMEGA EP short pulse and the cone target. The wire frame represents the view of the cone-wire target from the x-ray pinhole camera. The cone wall is thick enough to attenuate the x-rays totally.

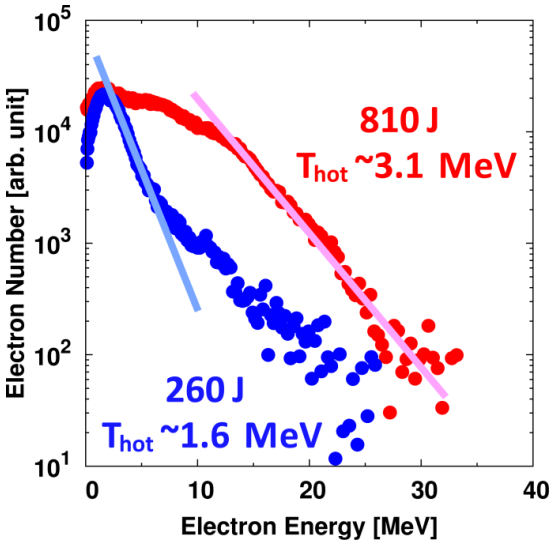

Figure 6. Vacuum electron energy spectra observed on the laser axis at OMEGA EP in the shot with laser energies of 810 J (260 J) shown with red (blue) dots.

potential [30] ($T_{\mathrm{pond}} \approx 0.3$ and 0.5 MeV, respectively), which is a characteristic of electrons accelerated in underdense plasma [31].

It should be noted that the effect of preplasma presence inside the cone in the laser interactions was also previously investigated by MacPhee *et al* [13] using Cu cones with the Titan laser and PIC simulations. They found that the preplasma produced with a 100 mJ prepulse reduced the number of forward going fast electrons with energies 2–4 MeV. In these

PIC simulations, the Cu plasma cone target including the preplasma was modeled with a fixed ionization level. However, strong laser heating in the LPI will cause local increases in plasma ionization. Therefore, inclusion in PIC codes of a dynamic ionization capability becomes important especially for high Z materials such as gold, which has been considered for the cone material in the FI. In the following sections, we describe the numerical investigation of LPI and fast electron generation and energy coupling in cone-wire targets with different scale-length preplasmas including time-varying ionization by field and collisional ionization.

4. Collisional particle-in-cell modeling using the PICLS code

4.1. PICLS simulations to determine the effects of preplasma

Collisional PIC simulations were performed using the PICLS [32] code to examine the underlying physics of the laser matter interactions and fast electron transport. In the first simulations, in two dimensions (2D), a semi-infinite Gaussian (spatial and temporal) laser pulse with rise in $100\tau_L(\tau_L = 3.3\,\text{fs})$ followed by a constant power was injected into cone-wire targets with the focused spot diameter of 40 μm. The peak laser intensity was $I_{peak} \sim 4 \times 10^{18}\,\text{W cm}^{-2}$ and the wavelength (λ_L) was 1 μm. The cone and the wire were plasmas with the density of solid gold ($19.7\,\text{g cm}^{-3}$) and copper ($8.94\,\text{g cm}^{-3}$), respectively. The ion density for Au (Cu) is set to $53n_c(76n_c)$ according to its mass density, where n_c is the critical density for 1 μm wavelength light. The initial ionization state is set to +10 (+3) for Au (Cu). The simulations use a spatial (temporal) resolution of $\lambda_L/60$ ($\tau_L/60$) and the number of particles per cell used was 29. Initially all particles are at rest with the plasma temperature set to zero. Absorbing boundary conditions are applied for fields and particles (i.e. no fast electrons re-circulated back into the target). The ionization charge states of ion species are calculated with an electron impact collisional ionization model. Due to computational limitations the preplasma scale length and the laser pulse duration in simulations were reduced to $L = 15\,\mu$m and $\tau \approx 1\,$ps compared to the experimental conditions which were $L \approx 35\,\mu$m and $\tau = 10\,$ps, respectively.

To demonstrate the effect of different preplasma scale lengths on laser energy coupling to the wire, another similar PICLS run was performed with a 5× shorter preplasma scale length, i.e. $L = 3\,\mu$m. Simulation target electron density profiles are shown in figure 7(a) for $L = 15\,\mu$m (upper half), $L = 3\,\mu$m (lower half), here X and Y are longitudinal and transverse dimensions. The laser pulse enters through the left boundary and illuminates the target at normal incidence. Figures 7(b) and (c) show the cycle averaged (quasi-static) azimuthal magnetic field at 1 ps for $L = 15$ and $3\,\mu$m, respectively; the positions of $X \sim 40\,\mu$m ($L = 15\,\mu$m) and $X \sim 55\,\mu$m ($L = 3\,\mu$m) correspond to the relativistically corrected critical density region where the laser pulse has stopped and effectively generates the fast electrons. As shown in figure 7(d), the fast electron energy density is maximum at the position where the laser pulse stops propagating. In the $L = 15\,\mu$m case, the laser energy coupling occurs at a significant offset distance from the wire, while in the $L = 3\,\mu$m case the laser interaction takes place near the cone tip. The time integrated fast electron flux, collected through a 2 μm wide observation box behind the cone tip, shows that twice as many electrons reach the wire in the shorter preplasma case. We further compared the energy deposited in the Cu wire via spatial integration of bulk (background) electron energy in the first 5 μm of the wire length, see figure 7(e), which clearly shows that the existence of longer preplasma significantly reduces the energy coupling to the wire. Note here that the simulations compare the coupling reduction in $L \approx 15\,\mu$m with small preplasma of

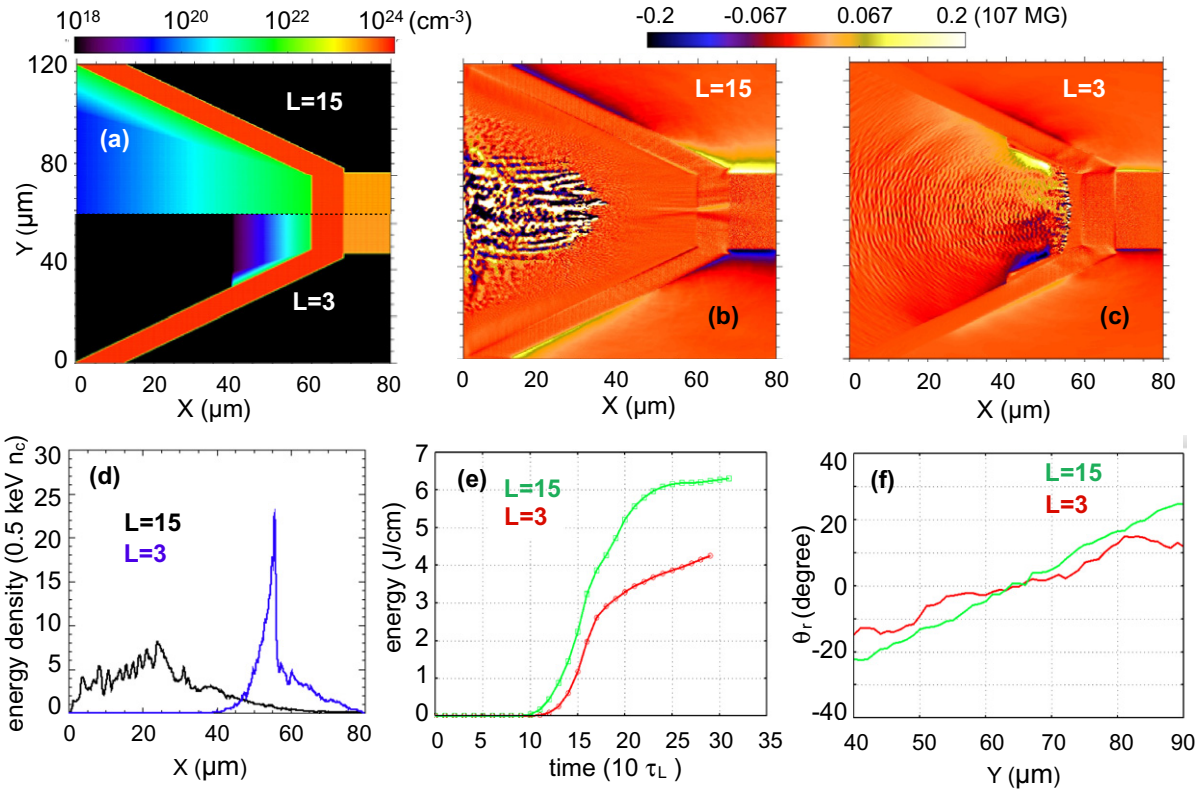

Figure 7. PICLS (a) target densities for $L = 15\,\mu$m (upper half) and $L = 3\,\mu$m (lower half), (b) simulation results showing magnetic field (B_z) in the cases of (b) $L = 15\,\mu$m and (c) $L = 3\,\mu$m scale length. The field is averaged over a laser cycle. The values shown in the figures indicate the maximum field strength. (d) Energy density of fast electrons along the wire axis in two cases (e) energy evolution of bulk electrons in Cu wire with time. (f) Mean propagation angle compared for two scale length cases.

$L \approx 3\,\mu$m, however experimentally observed coupling reduction at OMEGA EP for preplasma scale ($L \sim 35\,\mu$m) will be discussed in section 4.3.

This reduction can be attributed to multiple important effects occurring in the LPI region. First the offset distance of time-evolved critical surface from the cone tip during the laser interaction is larger in the $L = 15\,\mu$m case as compared to the $L = 3\,\mu$m case. Since the fast electron beam has an angular divergence associated with it, a larger offset distance of electron source reduces the flux received by the wire with a limited diameter ($\sim$30 μm in our simulations). Second is the effect of long scale preplasma on electron beam divergence; as discussed by Debayle *et al* [33], electrons accelerated in a larger volume tend to have a wider divergence. This effect is consistent with our simulations as follows. For these two different scale lengths ($L = 15$ and $3\,\mu$m), fast electron mean propagation angle ($\theta_r = \tan^{-1}(P_y/P_x)$), averaged over all particles was estimated a few microns beyond where the laser has stopped. When we plot the time integrated transverse distribution of θ_r as shown in figure 7(f), we observed that within the central 10 μm the θ_r is not much different for both cases, however in the $L = 15\,\mu$m case θ_r can be twice as large compared to the $L = 3\,\mu$m case in the region slightly away from the center (e.g. $Y \sim$ 55–60 and $\sim$70–75 μm); which indicates a relatively

more divergent electron beam. The cumulative effect of the larger offset distance of source and a more divergent electron beam can explain the ~2× reduction of electron flux arriving at the wire in the longer preplasma case as detailed below.

4.2. Numerical analysis of fast electron transport

Next, we discuss the results obtained with a simple numerical model estimation that predicts the number of electrons that will reach the wire based on their properties at the source. The prediction can be compared to the actual simulation result to determine whether or not electron trajectories were altered between the source and the cone. The model uses the simulation electron momentum information ($P(x, y, z, t)$) in an extraction box (say, at (x_s, y)) near the electron source to predict the number of electrons ideally reaching the wire tip (say, (x_p, y)). This model basically integrates electron flux distribution ($n_e(x_{s,} y)$), near the source but only including those electrons whose energy is greater than 10 keV and projected transverse coordinate (y_p) at the wire tip plane, as determined by each one's propagation angle, lies within the wire width (W); $N_e = \int_{y_p=l_1}^{y_p=(l_1+W)} n_e(x_s, y)\,dy$, where y_p is defined as $y_p = \tan\theta_r X_{offset} + y$ and l_1 and $(l_1 + W)$ are the transverse coordinates of the wire's lower and upper edges. X_{offset}, which is the distance between the extraction box near the source and the wire tip, is 25 and 10 μm for $L = 15$ and 3 μm cases, respectively. Based on electron source offset distance and angular divergence the model predicts that ~2× as many electrons should reach the wire in the $L = 3\,\mu$m case. Further, we assume a 2 μm wide box at the wire tip and count the number of electrons passing through the box and actually entering the wire in the simulation and again found the 2× increase in the $L = 3\,\mu$m case. Note that the consistency of these results also suggests that there is no anomalous stopping of electrons during their transport from the source to the wire in the longer preplasma case. This enables us to use this model to estimate the electron flux reduction for actual experimental conditions.

4.3. Comparison to full-scale, 10 ps experiments

As mentioned above, for the OMEGA EP experiment the HYDRA predicted preplasma scale was $L \approx 35\,\mu$m; using this scale length the offset distance of the relativistic critical density position (or electron source) from the cone tip was estimated to be ~100 μm. Using the above mentioned model, we then extrapolate the reduction factor for experimentally produced preplasma conditions ($L = 35\,\mu$m and $X_{offset} \sim 100\,\mu$m) assuming similar electron source characteristics and observed a 7–8 times reduction in electron flux reaching the wire compared to a small preplasma case. This estimation is found to be consistent with experimentally observed coupling reduction in the EP experiment compared to Titan results for identical targets but with ~60 times less prepulse energy associated with the Titan laser pulse.

Note that due to computational limitations, PICLS modeling was only performed for a reduced time scale of 1 ps, whereas the experiment time scale was ~10 ps. However, even with the limited modeling results we have demonstrated that the higher level of pre-pulse will deteriorate the energy coupling to the wire, which is in qualitative agreement with the experimental observation. For a better description and quantitative interpretation of FI relevant experiments, modeling of laser interaction with cone targets for FI relevant time scale (~10 ps) is very important. There may exist other interesting physics effects, which were not observed with 1 ps interaction. Some of the interesting features such as strong laser focusing and hosing

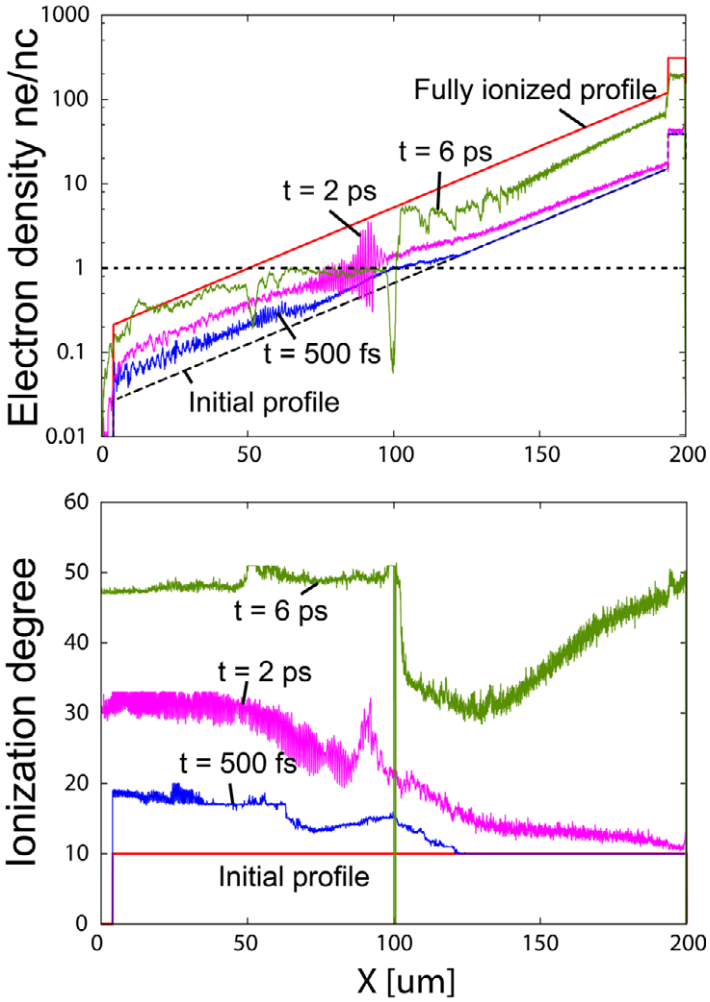

Figure 8. Results of PICLS simulation in 1D including dynamic ionization process. (a) Temporal evolution of the density profile of preplama that has the initial scale length of 30 μm. (b) Ionization level of the gold plasma at the same timing as plot (a). Initial ionization level was 10 in the whole region of the plasma.

instability have been observed during the intense laser ($I_{\text{peak}} \sim 4 \times 10^{20}\,\text{W cm}^{-2}$) interaction with the Cu cone over a few picoseconds [13].

4.4. Effects of dynamic ionization on laser plasma interaction

Finally, to investigate the effect of including dynamic ionization on the preplasma density profile during laser irradiation, we performed a simulation using PICLS in one dimension (1D) with the gold ionization dynamics described by field ionization [34] and a fast electron collisional ionization model [35]. The collisional ionization model imposes significant numerical costs at the full spatial scale. Therefore, the domain is limited to 1D for this study. For simplicity, the initial ionization level in the whole region of preplasma (30 μm scale length) was set as $Z = 10$, which was the averaged ionization level in HYDRA calculations. The laser pulse had a duration

of 10 ps and reached the peak intensity of 10^{19} W cm^{-2} at $t = 6$ ps. The temporal evolution of the plasma density profile and ionization level is shown in figure 8. Even in the first 500 fs period, the low density plasma starts being ionized primarily via field ionization, which moves the critical density position towards the left. Meanwhile, the plasma is also pushed towards the right side due to the laser ponderomotive force. The motion of the critical density position is a balance of those two effects and the relativistic correction varies with the laser intensity, also, in time. Combining those effects, the simulation shows that the critical density position advances away from the initial solid surface with a speed of $0.05c$ until the laser intensity reaches about half of its peak ($t = 3$ ps). At which time, the critical density position has shifted by 40 μm, adding 30% to the initial 130 μm travel distance for fast electrons from the critical density position to the cone tip. As we discussed above, such extension of the transport distance of the fast electrons in the preplasma affects and reduces the coupling efficiency of the fast electrons significantly. At later times, the simulation shows that the critical density position is pushed back towards higher density due to larger ponderomotive force. Such motions of the critical surface on the timescale of the laser pulse have recently been diagnosed experimentally [36]. However, in our simulations the net effect was that the critical density position returned nearly to the original point, about 100 μm away from the target surface, which is long enough to cause a significant energy loss of the fast electron energy in the preplasma with higher density than the initial one. Finally, the ionization level reached $\sim$35 in the vicinity of the critical density position at the timing of the peak intensity.

It is worth noting that the calculated frequency of collisional ionization was $\sim 10^{12}$ s^{-1} at the critical density region and it is even higher in the over-dense region. This indicates that the dynamic ionization is important for laser pulses longer than a few picoseconds, such as full scale FI-related lasers; a slower laser intensity rise time would result in a larger excursion of the critical surface position. It should also be noted that the dynamic ionization effect due to the intense laser irradiation is more significant for higher Z material. For low Z material, the preplasma can be almost fully ionized when it is created by the prepulse, so that the change of the plasma density profile upon irradiation can be small even when the plasma is heated by the intense laser pulse and fast electrons.

5. Summary

In summary, the results clearly suggest that for full scale FI experiments with > 10 kJ, 10 ps class lasers, prepulse affects the laser energy coupling into fast electrons and consequently to the compressed core. With the help of PIC simulations we have demonstrated that large scale preplasma in the cone for integrated FI experiments could be a serious issue and reduces the coupling of the fast electrons to the compressed core significantly. Note that although 2D PICLS simulations are performed with limited scale, they present qualitative agreement with the experimental observation. The coupling reduction is more important for cones made of high Z materials. In high Z material such as gold ($Z = 79$), the dynamic ionization of preplasma by intense laser heating will cause a significant increase in local electron density profile and consequently push the electron source position farther away from the cone tip. Limiting the prepulse using a high contrast laser pulse to avoid the creation of large scale preformed plasma inside the reentrant cone or use of a relatively low-Z material, such as Al, for the cone interior is recommended [37].

Acknowledgments

The work was supported by NNSA/US DOE under contract numbers DE-FG52-09NA29033 (NLUF), DE-FC02-04ER54789 (FSC), and DE-FG02-05ER54834 (ACE). DB and LAG acknowledge financial support from the HiPER project for their participation in the experiment at Omega-EP.

References

[1] Tabak M *et al* 1994 *Phys. Plasmas* **1** 1626
[2] Tabak M *et al* 2006 *Fusion Sci. Technol.* **49** 254
[3] Pukhov A and Meyer-ter-Vehn J 1997 *Phys. Rev. Lett.* **79** 2686
[4] Tanaka K A *et al* 2000 *Phys. Plasmas* **7** 2014
[5] Kodama R *et al* 2001 *Phys. Plasmas* **8** 2268
[6] Kodama R *et al* 2002 *Nature* **418** 933
[7] Theobald W *et al* 2011 *Phys. Plasmas* **18** 056305
[8] Ma T *et al* 2012 *Phys. Rev. Lett.* **108** 115004
[9] Baton S D *et al* 2008 *Phys. Plasmas* **15** 042706
[10] King J A *et al* 2009 *Phys. Plasmas* **16** 020701
[11] Green J S *et al* 2007 *Nature Phys.* **3** 853
[12] Van Woerkom L *et al* 2008 *Phys. Plasmas* **15** 056304
[13] MacPhee A G *et al* 2010 *Phys. Rev. Lett.* **104** 055002
[14] Meyerhofer D D *et al* 2010 *J. Phys.: Conf. Ser.* **244** 032010
[15] Kemp A J and Divol L 2012 *Phys. Rev. Lett.* **109** 195005
[16] Nilson P M *et al* 2010 *Phys. Rev. Lett.* **105** 235001
[17] Key M H *et al* 2008 *Phys. Plasmas* **15** 022701
[18] Mima K *et al* 2010 *Plasma Phys. Control. Fusion* **52** 124047
[19] Chrisman B, Sentoku Y and Kemp A J 2008 *Phys. Plasmas* **15** 056309
[20] Kemp A J *et al* 2009 *Phys. Rev.* E **79** 066406
[21] Baton S D *et al* 2007 *High Energy Density Phys.* **3** 358
[22] Sentoku Y *et al* 2004 *Phys. Plasmas* **11** 3083
[23] Cao L *et al* 2008 *Phys. Rev.* E **78** 036405
[24] Perkins L J *et al* 2000 *Nucl. Fusion* **40** 1
[25] Kodama R *et al* 2004 *Nature* **432** 1005
[26] Akli K U *et al* 2010 *J. Instrum.* **5** P07008
[27] Marshall F J *et al* 2001 *Rev. Sci. Instrum.* **72** 713
[28] Chen H *et al* 2008 *Rev. Sci. Instrum.* **79** 10E533
[29] Marinak M *et al* 1998 *Phys. Plasmas* **5** 1125
[30] Wilks S C 1993 *Phys. Fluids* **5** 2603
[31] Paradkar B S *et al* 2011 *Phys. Rev.* E **83** 046401
[32] Sentoku Y and Kemp A J 2008 *J. Comput. Phys.* **227** 6846
[33] Debayle A *et al* 2010 *Phys. Rev.* E **82** 036405
[34] Kato S, Kishimoto Y and Koga J 1998 *Phys. Plasmas* **5** 292
[35] Lotz W 1970 *Z. Phys.* **232** 101
[36] Ping Y *et al* 2012 *Phys. Rev. Lett.* **109** 145006
[37] Solodov A A *et al* 2012 *42nd Annu. Conf. on Anomalous Absorption* (*Key West, FL*)